ACS APPLIED MATERIALS & INTERFACES

Research Article

www.acsami.org

An Effective Approach for Alleviating Cation-Induced Backbone Degradation in Aromatic Ether-Based Alkaline Polymer Electrolytes

Juanjuan Han,[†] Qiong Liu,[†] Xueqi Li,[†] Jing Pan,*[,†] Ling Wei,[†] Ying Wu,[†] Hanqing Peng,[†] Ying Wang,[†,‡] Guangwei Li,[†] Chen Chen,[†] Li Xiao,[†] Juntao Lu,[†] and Lin Zhuang*[,†,‡]

[†]College of Chemistry and Molecular Sciences, Hubei Key Lab of Electrochemical Power Sources, and [‡]Institute for Advanced Studies, Wuhan University, Wuhan 430072, China

Supporting Information

ABSTRACT: Aromatic ether-based alkaline polymer electrolytes (APEs) are one of the most popular types of APEs being used in fuel cells. However, recent studies have demonstrated that upon being grafted by proximal cations some polar groups in the backbone of such APEs can be attacked by OH^-, leading to backbone degradation in an alkaline environment. To resolve this issue, we performed a systematic study on six APEs. We first replaced the polysulfone (PS) backbone with polyphenylsulfone (PPSU) and polyphenylether (PPO), whose molecular structures contain fewer polar groups. Although improved stability was seen after this change, cation-induced degradation was still obvious. Thus, our second move was to replace the ordinary quaternary ammonia (QA) cation, which had been closely attached to the polymer backbone, with a pendant-type QA (pQA), which was linked to the backbone through a long side chain. After a stability test in a 1 mol/L KOH solution at 80 °C for 30 days, all pQA-type APEs (pQAPS, pQAPPSU, and pQAPPO) exhibited as low as 8 wt % weight loss, which is close to the level of the bare backbone (5 wt %) and remarkably lower than those of the QA-type APEs (QAPS, QAPPSU, and QAPPO), whose weight losses under the same conditions were >30%. The pQA-type APEs also possessed clear microphase segregation morphology, which led to ionic conductivities that were higher, and water uptakes and degrees of membrane swelling that were lower, than those of the QA-type APEs. These observations unambiguously indicate that designing pendant-type cations is an effective approach to increasing the chemical stability of aromatic ether-based APEs.

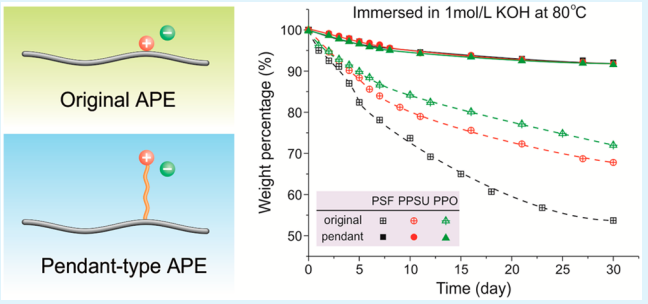

KEYWORDS: *alkaline polymer electrolyte, chemical stability, backbone degradation, pendant-type quaternary ammonia cation, phase separation, fuel cell application*

INTRODUCTION

Proton exchange membrane fuel cells (PEMFCs) are an advanced electrochemical power source possessing many advantages, including a compact structure, room-temperature startup capacity, and high power density, which makes them ideal for vehicle and portable applications.[1−4] However, the strongly acidic polyelectrolyte used in PEMFCs restricts the choice of catalyst to only the noble metals, and Pt in particular, which has been a major obstacle preventing the widespread deployment of PEMFCs.[5−9] To address this platinum-dependence issue while maintaining the advantages of PEMFCs, a new class of fuel cells, alkaline polymer electrolyte fuel cells (APEFCs), was proposed.[10−13] Replacing the proton exchange membrane (PEM) with an alkaline polymer electrolyte (APE) allows some nonprecious metals to be used as the electrode catalyst.[14−18] In the past decade, great efforts have been devoted to the realization of APEFCs and to the development of high-performance APEs in particular.[19−27]

For fuel cell applications, the APE should be of high physical and chemical quality (i.e., not only the ionic conductivity and mechanical strength but also the chemical stability should be as high as possible). It is not easy, however, to find an APE that fulfills all of these requirements. During the past decade, the physical qualities of APEs, including their ionic conductivity and mechanical properties, have been greatly improved;[28−36] however, the chemical stability of APEs remains an issue. Although instability of the organic cation, mostly quaternary ammonia, has been well recognized and is the focus of much research,[37−42] the polymer backbone problem was somewhat unexpected and has just recently been realized.[43,44]

On the basis of NMR analyses, Arges and co-workers recently found that, although the polysulfone (PS) backbone itself is stable in hot, concentrated KOH solutions, quaternary ammonium polysulfone (QAPS) degraded significantly via quaternary carbon hydrolysis and ether hydrolysis (Figure S1 in the Supporting Information) in 1 or 6 mol/L KOH solutions at 60 °C.[43] This observation indicates that the cation grafted closely to the backbone has greatly altered the chemical

Received: November 18, 2014
Accepted: January 16, 2015
Published: January 16, 2015

DOI: 10.1021/am508009z
ACS Appl. Mater. Interfaces 2015, 7, 2809−2816

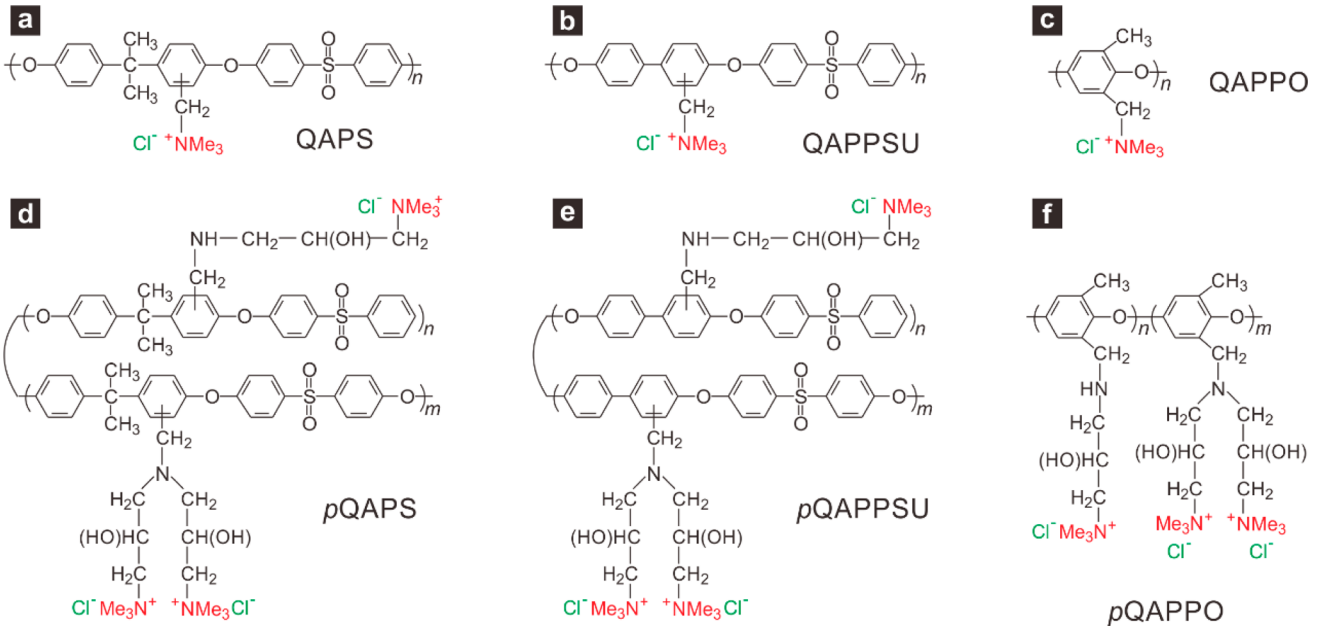

Figure 1. Chemical structures of the APEs studied herein: (a) QAPS, (b) QAPPSU, (c) QAPPO, (d) pQAPS, (e) pQAPPSU, and (f) pQAPPO.

properties of the polymer. Our previous study also showed that reducing the degree of grafting, such as by designing double cations on the side chain, can effectively improve the stability of QAPS.[19]

Here, we report a systematic study on the backbone stability of six aromatic ether-based APEs involving three types of backbone and two types of cation. In addition to PS, polyphenylsulfone (PPSU) and polyphenylether (PPO) are employed as the polymer backbone (Figure 1) with gradually simplified molecular structures: PS contains both propyl and sulfone groups, PPSU has no propyl groups, and PPO does not have propyl or sulfone groups. This sequence of polymers should provide a clear observation of the weak points of the backbone under alkaline conditions. To investigate the cation-induced degradation, two types of quaternary ammonia are compared: the original (Figure 1a–c) and pendent (Figure 1d–f) type. The former is attached closely to the backbone, whereas the latter is linked to the backbone via a long side chain in which the cation–backbone interaction is expected to be significantly weakened.

EXPERIMENTAL SECTION

Materials. Polysulfone (Udel P-3500, Solvay Advanced Polymers, LLC), polyphenylsulfone (Radel R-5500, Solvay Advanced Polymers, LLC), poly(phenylene oxide) (MW = 30000 g/mol, Sigma-Aldrich), chloromethyl methyl ether (Shanghai Quhua Chemical Reagent Co. Ltd., 99%), trifluoroacetic acid (Sinopharm Chemical Reagent Co. Ltd., 99%), zinc powder (Shanghai Chemical Reagent Co. Ltd., 95%), zinc chloride (Sinopharm Chemical Reagent Co. Ltd., 98%), *N*-bromosuccinimide (Sinopharm Chemical Reagent Co. Ltd., 99%), azobis(isobutyronitrile) (Shanghai Sihewei Chemical Industry Co. Ltd., 80%), 1,2-dichloroethane (Shanghai Chemical Reagent Co. Ltd., 99%), 1,1,2,2-tetrachloroethane (Sinopharm Chemical Reagent Co. Ltd., 98%), dichloromethane (Sinopharm Chemical Reagent Co. Ltd., 99%), chlorobenzene (Sinopharm Chemical Reagent Co. Ltd., 99.5%), chloroform (Sinopharm Chemical Reagent Co. Ltd., 99%), trimethylamine (Sinopharm Chemical Reagent Co. Ltd., 33% alcohol solution), glycidyltrimethylammonium chloride (Shanghai Dibai Chemical Reagent Co. Ltd., 95%), ammonia solution (Shanghai Chemical Reagent Co. Ltd., NH_3 content of 25–28 wt %), *N*,*N*-dimethylformamide (DMF, Sinopharm Chemical Reagent Co. Ltd., 99.5%), dimethyl sulfoxide (DMSO, Sinopharm Chemical Reagent Co. Ltd., 99%), methanol (Sinopharm Chemical Reagent Co. Ltd., 99.5%), ethanol (Sinopharm Chemical Reagent Co. Ltd., 99.7%), potassium hydroxide (Sinopharm Chemical Reagent Co. Ltd., 85%), and hydrochloric acid (Sinopharm Chemical Reagent Co. Ltd., 37%) were all used as received.

Synthesis and Characterization of Long-Chain Quaternary Ammonia. Two long-chain quaternary ammonia, 1-amino-2-hydroxy-3-trimethylammonium propane chloride (SQA), and *N*,*N*-di(2-hydroxy-3-trimethylammonium propane chloride) amine (DQA) were applied in this work. The synthetic process and characterizations are as follows. Glycidyl trimethylammonium chloride (GTMAC, 4 g) was dissolved in water (20 mL) to form a solution, which was later added to an ammonia solution (13.2 mL) at room temperature. The reaction mixture was then stirred for 4 h at 40 °C. After the reaction, the solvent and excess ammonia were removed on a rotary vacuum evaporator at 50 °C to yield a mixture of SQA and DQA (Scheme 1).

Scheme 1. Reaction Process for SQA and DQA

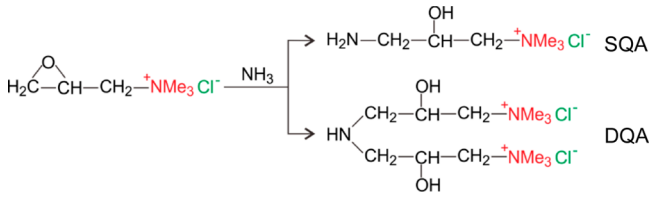

^{1}H NMR (300 MHz) analysis was performed on a Varian Mercury VX-300 spectrometer using deuterated dimethyl sulfoxide (d^6-DMSO) as the solvent and tetramethylsilane (TMS) as the internal reference. ^{1}H NMR (300 MHz, d^6-DMSO) for SQA ($[NH_2CH_2CH(OH)CH_2N(CH_3)_3]^+Cl^-$) and DQA ($([CH_2CH(OH)CH_2N(CH_3)_3]^+Cl^-)_2NH$): δ 5.6–5.7 ppm, 2H (NH_2- in SQA); δ 4.0–4.3 ppm, 2H (-*CH*(OH)- in SQA and DQA); δ 3.5–3.6 ppm, 3H (-CH(*OH*)- in SQA and DQA); δ 3.4–3.5 ppm, 3H, and δ 3.2–3.3 ppm, 3H ($-CH_2N^+(CH_3)_3$ in SQA and DQA); δ 3.26 ppm, 26H ($-N^+(CH_3)_3$ in SQA and DQA); δ 2.5–2.8 ppm, 6H ($-NH_2CH_2-$ in SQA and $-NH(CH_2)_2-$ in DQA); and δ 1.94 ppm, 1H (-*NH*- in DQA).

Electrospray Ionization–Mass Spectrometry (ESI–MS). ESI–MS of SQA and DQA measurements were performed on a Finnigan LCQ advantage instrument. Peaks emerged at m/z = 301.1 and 284.2

DOI: 10.1021/am508009z
ACS Appl. Mater. Interfaces 2015, 7, 2809–2816

corresponding to $[SQA^+-SQA^+Cl^-]^+$ and $[DQA^{2+}Cl^-]^+$, respectively (Figure S2 in the Supporting Information).

Elemental Analysis. Elemental analyses were performed on a Vario EL III elemental analyzer to determine the molar ratio of SQA to DQA. The weight percentages of elements C, H, and N were found to be 43.99, 9.86, and 14.2%, respectively. Thus, the molar ratio of SQA to DQA was calculated to be 1:1.

Synthesis of Chloromethyl Polysulfone (CMPS). The CMPS used in this study was synthesized following a procedure we reported previously.[10] The chloromethylation process of PS was carried out in a three-neck round-bottom flask with a mechanical stirrer. PS (10 g) was dissolved in 1,2-dichloroethane (70 mL). After zinc powder (1 g) and trifluoroacetic acid (4 mL) were added to the solution, chloromethyl methyl ether (20 mL) was added dropwise. The solution was stirred for 5 h at 30 °C. The chloromethylated polysulfone that was obtained was precipitated in methanol, washed several times with deionized water, and then dried in a vacuum oven for 24 h at 60 °C.

Synthesis of Chloromethyl Polyphenylsulfone (CMPPSU). PPSU (4 g) was dissolved in 120 mL of 1,1,2,2-tetrachloroethane to form a solution. Anhydrous zinc chloride (1.32 g) and chloromethyl methyl ether (34 mL) were then added in sequence. The mixture solution was stirred for 4 days at 55 °C. The obtained product mixture was precipitated in methanol, dissolved in dichloromethane, and precipitated in methanol again to obtain the final product, which was then washed several times with deionized water and dried in a vacuum oven for 24 h at 60 °C.

Synthesis of Brominated Poly(phenylene oxide) (BPPO). PPO (5 g) was dissolved in 40 mL of chlorobenzene to form a solution; then, azobis(isobutyronitrile) (0.84 g) and *N*-bromosuccinimide (14.8 g) were added slowly to the solution and stirred for 4 h at 130 °C under reflux. The mixture product was cooled to room temperature and precipitated in ethanol, dissolved in chloroform, and again precipitated in ethanol. The final product was washed several times with deionized water and then dried in a vacuum oven for 24 h at 60 °C.

Preparation of QA-Type APE Membranes. Dried CMPS, CMPPSU, and BPPO powders were dissolved in DMF to form 10 wt % solutions. Trimethylamine was then added to these solutions and stirred for 0.5 h at 40 °C to produce QAPS, QAPPSU, and QAPPO solutions, respectively. The resulting APE solutions were cast onto clean, flat glass plates and dried in an oven at 55 °C for 24 h and then dried further in a vacuum oven at 80 °C for 10 h. To replace the Cl^- anion with OH^-, the membranes were immersed in a 1 mol/L KOH solution for 10 h. This process was repeated four times to ensure complete displacement. Finally, the APE membranes with the OH^- anions were rinsed repeatedly with deionized water until the pH of the residual water was neutral.

Preparation of pQA-Type APE Membranes. Dried CMPS, CMPPSU, and BPPO powders were dissolved in DMSO to form 10 wt % solutions. A mixture of SQA and DQA was then added to these solutions and stirred for 3 h at 50 °C to produce solutions that were then cast onto clean, flat glass plates and dried in an oven at 85 °C for 24 h and then dried further in a vacuum oven at 80 °C for 10 h. To replace the Cl^- anion with OH^-, the membranes were immersed in a 1 mol/L KOH solution for 10 h. This process was repeated four times to ensure complete displacement. Finally, the pQA-type APE membranes with OH^- anions were rinsed repeatedly with deionized water until the pH of the residual water was neutral.

UV−Vis Spectroscopy Observations. UV−vis measurements were conducted on a Mapada UV-6100PC spectrometer. A clean KOH solution was used as the reference for the detection of degraded APE backbone fragments in the KOH solution.

Thermogravimetric Analysis (TGA). TGA was performed on a TGA Q500 (TA Instruments) thermogravimetric analyzer using samples (5 mg) placed in an Al_2O_3 crucible. The samples were heated from 30 to 600 °C at a rate of 5 °C/min under flowing air (40 mL/min).

Ion Exchange Capacity (IEC) Determinations. The IEC of APE was determined by titration. A membrane (OH^- form) was immersed in a standard hydrochloric acid solution (0.1 mol/L, 30 mL) for 48 h. The solution was then titrated with a standard solution of potassium hydroxide (0.1 mol/L) to pH 7. The membrane was washed and immersed in deionized water for 24 h to remove any residual HCl, and it was then dried under vacuum at 45 °C for 24 h and weighed to determine the dry mass (Cl^- form). The IEC of the membrane is calculated by

$$\mathrm{IEC} = \frac{n_{i(H^+)} - n_{f(H^+)}}{m_{dry(Cl^-)}} \quad (1)$$

where $n_{i(H^+)}$ and $n_{f(H^+)}$ are the initial and final amounts of proton in the HCl solution, respectively, as determined by titration, and $m_{dry(Cl^-)}$ is the mass of the dry membrane in the Cl^- form.

Ionic Conductivity Measurements. The OH^- conductivity of fully hydrated membranes with different IECs was measured at 60 °C using AC impedance spectroscopy (IviumStat). A membrane in the OH^- form was cut into 2 × 2 cm^2 pieces and sandwiched between two electrodes made of Teflon-bounded carbon film. The membrane resistance was measured under the open-circuit mode over a frequency range of 1 Hz to 1 MHz with an oscillating amplitude of 5 mV. The ionic conductivity was calculated as

$$\sigma = \frac{l}{R_{mem}A} \quad (2)$$

where l is the membrane thickness in cm, A the electrode area in cm^2, and R_{mem} the high-frequency resistance in Ω.

Swelling Degree Measurements. To obtain the swelling degree (denoted as s.d.%), we first recorded the dimensions of the dry membranes (Cl^- form, denoted as $x_{dry(Cl^-)}$). The membranes were then immersed in a 1 mol/L KOH solution for 48 h to convert Cl^- to OH^- and washed with deionized water several times to remove the remaining KOH. The dimensions of the membranes $x_{dry(OH^-)}$ could then be determined after wiping excess water from the surface. Accordingly, the s.d.% was calculated by

$$\text{s.d.\%} = \frac{x_{dry(OH^-)} - x_{dry(Cl^-)}}{x_{dry(Cl^-)}} \quad (3)$$

Transmission Electron Microscopy (TEM) Observations. An APE solution was cast to form a thin film on a Cu grid, which then exchanged the anions for I^- and was then subjected to TEM observations. Images were taken on an ultra-high-resolution transmission electron microscope (JEOL JEM-2010FEF) using an accelerating voltage of 200 kV.

Stability Tests. A piece of APE membrane (50 ± 3 μm in thickness) was immersed in a 1 mol/L KOH solution and maintained at 80 °C for 30 days. During the stability test, the KOH solution was sampled periodically for UV−vis detection. A signal in the range of 225−325 nm was due to the absorption of the phenyl group on the degraded fragment of the APE. After the 30-day test, the APE membrane was rinsed repeatedly with deionized water until the pH of the residual water was neutral, and the dried membrane was then weighed. The weight loss of the tested membrane was normalized by the signal strength of the final UV−vis spectrum, and then every UV−vis signal recorded during the electrolysis test could be converted to a value of weight loss. Meanwhile, the IEC and ionic conductivity of the APEs were tested before and after the stability test to evaluate the stability of cations under strong alkaline conditions.

RESULTS AND DISCUSSION

NMR Characterizations for the Synthesized APEs. Now that the mechanism of cation-induced backbone degradation for QAPS has been identified,[40] the strategy for addressing this issue may include two primary aspects, namely, removing the vulnerable polar groups from the PS backbone and moving the cation away from the polymer backbone. To test the effectiveness of these approaches, we chose three types of polymer backbones (i.e., PS, PPSU, and PPO) and attached them to two different cations (quaternary ammonium (QA)

DOI: 10.1021/am508009z
ACS Appl. Mater. Interfaces 2015, 7, 2809−2816

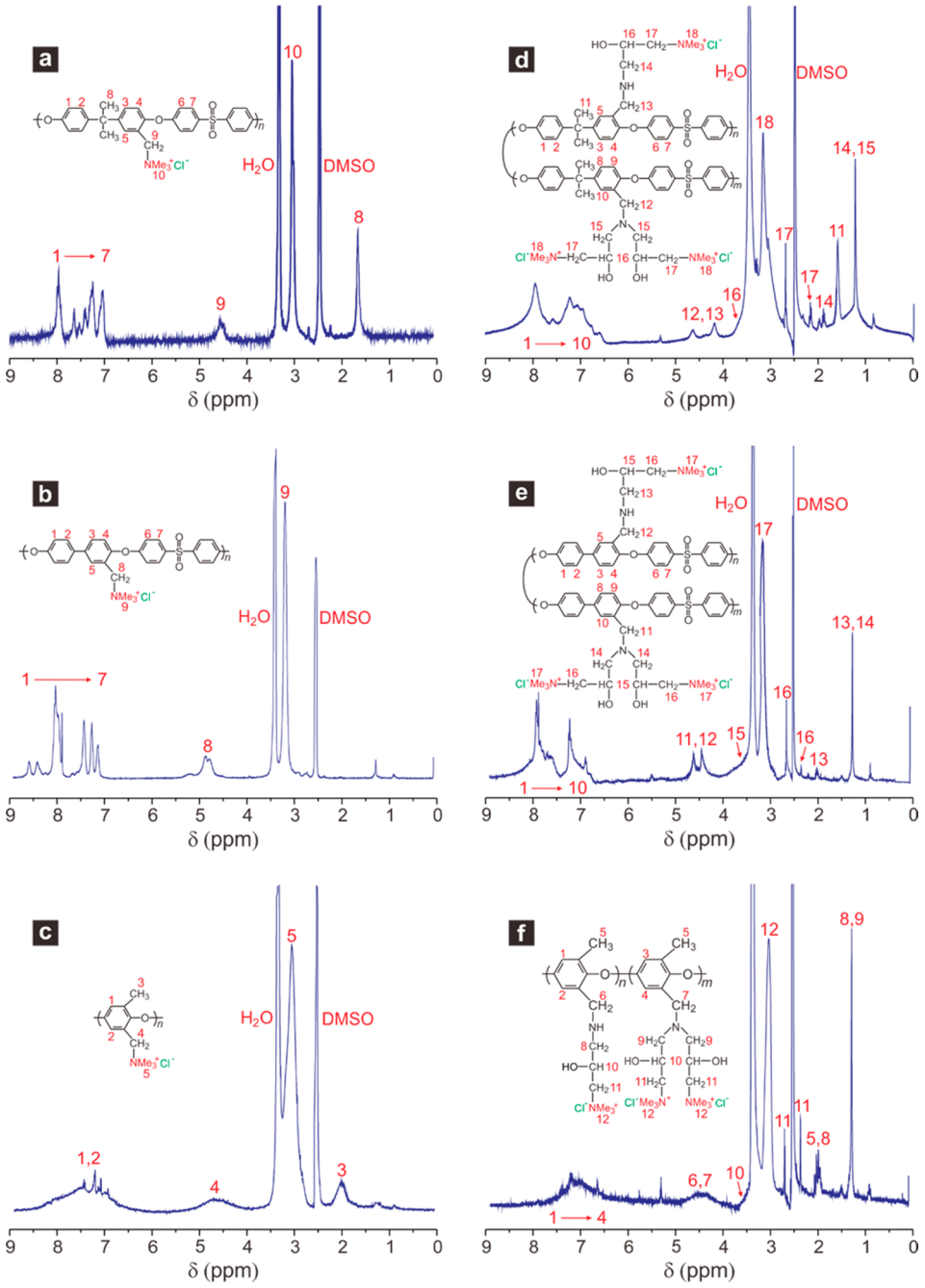

Figure 2. ^{1}H NMR spectra of synthesized APEs: (a) QAPS, (b) QAPPSU, (c) QAPPO, (d) pQAPS, (e) pQAPPSU, and (f) pQAPPO.

and pendant QA (pQA)). The six resulting APEs are designated QAPS, QAPPSU, QAPPO, pQAPS, pQAPPSU, and pQAPPO (Figure 1).

Prior to stability tests being performed, structural characterizations were conducted to ascertain the success of material syntheses. As indicated by the ^{1}H NMR results (Figure 2), there are four chemical environments for H atoms in QA-type APEs, and the peaks between 6.5 and 9.0 ppm correspond to H atoms in benzene rings. The single peak that emerges at 1.6 ppm is in response to the H in the methyl group of quaternary carbon in the backbone of QAPS, and the appearance of peaks at 4.5−5.0 ppm identifies H atoms of the benzyl group. More importantly, the peaks emerging at 3.1 ppm prove the existence of the QA ionic group in QAPS, QAPPSU, and QAPPO.

For the pQA-type APEs (pQAPS, pQAPPSU, and pQAPPO), the ^{1}H NMR spectra (Figure 2d−f) show new peaks corresponding to H atoms in the alkyl groups of the pendant side chains in addition to the signals for H atoms in the benzene ring (6.5−8.5 ppm), quaternary carbon (1.6 ppm), benzyl (4.0−5.0 ppm), and pQA groups (3.1 ppm).

Conducting Behavior of the Studied APEs. Ionic conductivity and water absorbing capacity are two key properties of APEs for fuel cell applications. As demonstrated in Figure 3a, the ion conductivity of pQA-type APEs is higher than that of QA-type APEs, which is understandable because the pQA-type APEs synthesized in this work all possess ion exchange capacities (IECs) that are higher than those of the QA-type APEs. Specifically, when the temperature is elevated from 20 to 80 °C, the conductivities of pQAPS (IEC = 2.01

DOI: 10.1021/am508009z
ACS Appl. Mater. Interfaces 2015, 7, 2809−2816

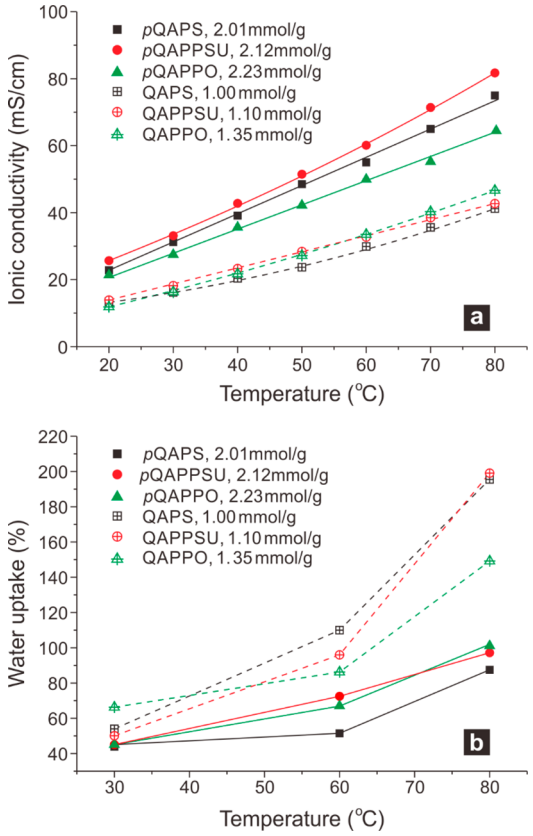

Figure 3. Ionic conductivity (a) and water uptake (b) of QA- and pQA-type APEs measured at different temperatures.

mmol/g), pQAPPSU (IEC = 2.12 mmol/g), and pQAPPO (IEC = 2.23 mmol/g) change from 22.8, 25.7, and 21.8 mS/cm to 73.7, 83.5, and 64.4 mS/cm, respectively. For comparison, the conductivities of QAPS (IEC = 1.00 mmol/g), QAPPSU (IEC = 1.10 mmol/g), and QAPPO (IEC = 1.35 mmol/g) change from 13.4, 13.9, and 12.2 mS/cm to 37.5, 40.5, and 46.5 mS/cm, respectively.

A very intriguing property of the pQA-type APEs is that even though their IECs are twice that of the QA-type APEs they absorb less water. As shown in Figure 3b, the water uptakes of pQAPS, pQAPPSU, and pQAPPO are just 87.5, 97.2, and 101.3%, respectively, compared to 195.5, 199.1, and 150.0% for QAPS, QAPPSU, and QAPPO, respectively. This unusual property of pQA-type APEs (i.e., higher IEC and ionic conductivity but lower water uptake) can be ascribed only to their morphological microphase separation feature.

X-ray diffraction analyses for the studied APEs indicated that they were all amorphous in nature; however, their morphologies turned out to be distinct as displayed by TEM images (Figure 4). The QA-type APEs have no clear microphase separation (Figure 4a–c), whereas the hydrophilic domain of the pQA-type APEs gets bigger and they aggregate to each other upon introduction of the long pQA side chain (Figure 4d–f). Such microphase separation morphology provides not only a strong hydrophobic frame to prevent excessive swelling upon water absorption but also broad, efficient ionic channels that enhance ionic conductivity.[28]

Chemical Stability of the Studied APEs. A chemical stability test of the studied APEs was performed in a hot alkaline solution (1 mol/L KOH solution at 80 °C) for 30 days. During the test, UV–vis spectroscopy was employed to detect degraded backbone fragments dissolved in the KOH solution (Figure 5a). Weight loss of the APEs as a function of time is

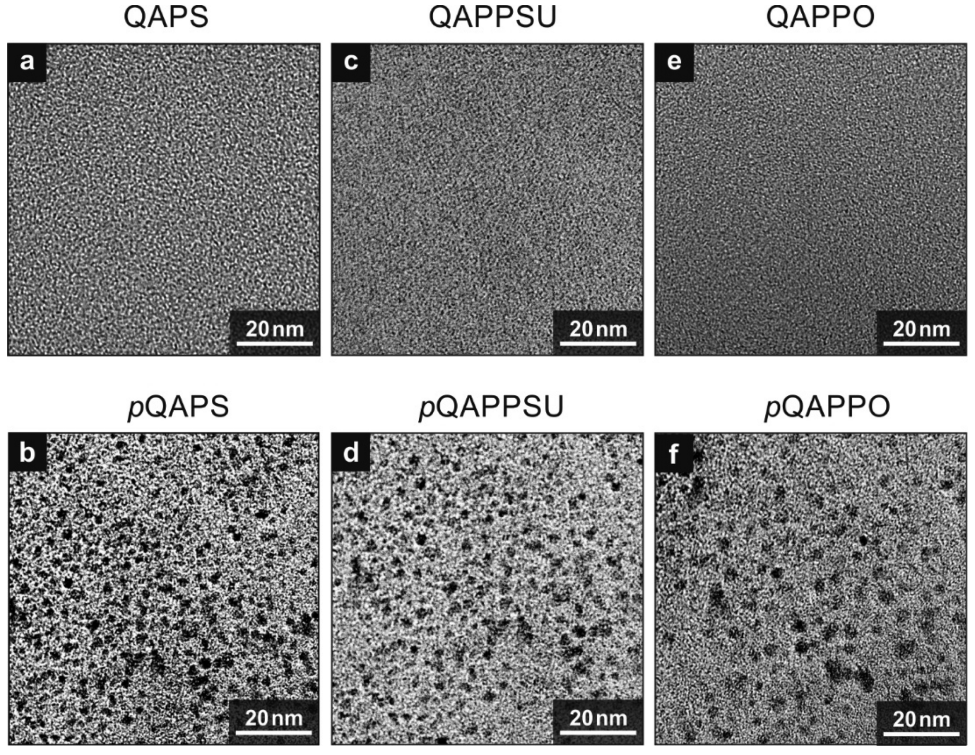

Figure 4. Transmission electron microscopy (TEM) images for the studied APEs: (a) QAPS, (b) QAPPSU, (c) QAPPO, (d) pQAPS, (e) pQAPPSU, and (f) pQAPPO. The dark spots in the images represent hydrophilic domains that have been dyed with iodine ions.

DOI: 10.1021/am508009z
ACS Appl. Mater. Interfaces 2015, 7, 2809–2816

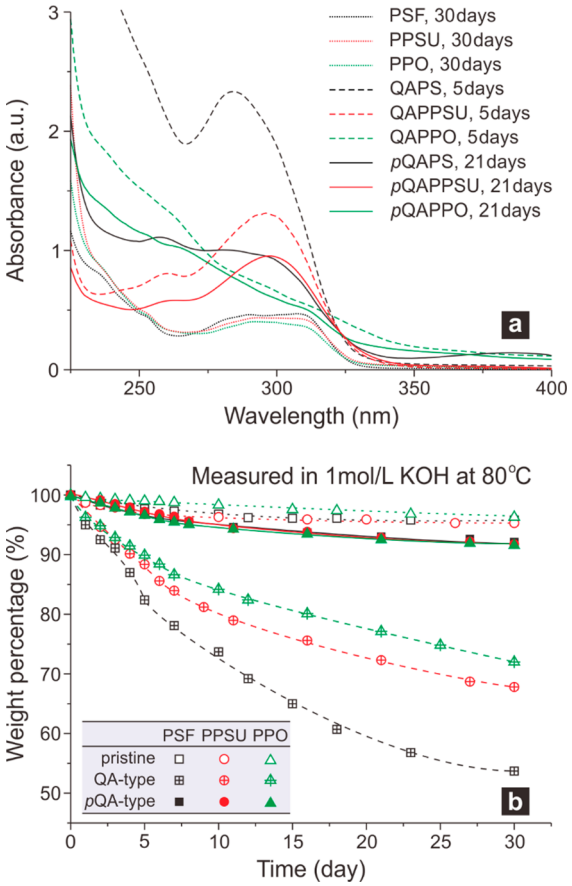

Figure 5. Stability test of the studied APEs in a 1 mol/L KOH solution at 80 °C. Pristine PS, PPSU, and PPO were also tested for reference. (a) Representative UV−vis spectra to be converted to weight loss of the polymers. (b) Weight loss of the studied APEs and their bare backbones as a function of time.

shown in Figure 5b. Clearly, the backbones of pristine polymers (PS, PPSU, and PPO) are quite stable under a strong alkaline environment, and at the 30th day their weight losses are all less than 5 wt %. However, when the QA group was attached closely to the polymer chains, the backbones of QAPS, QAPPSU, and QAPPO degraded at a notable rate. The most severe degradation was QAPS, which had a weight loss at the 30th day of 46 wt %, resulting in membrane cracking.

QAPPSU and QAPPO show stabilities that are somewhat higher than that of QAPS, which should be ascribed to the removal of polar groups, and the propyl group in particular, from their backbones. However, the backbone stability of QAPPSU and QAPPO is still not sufficient as the weight losses of QAPPSU and QAPPO at the 30th day were 32 and 28 wt %, respectively, indicating that even though the molecular structure of the polymer backbone had been greatly simplified, such as the PPO, its chemical properties are still altered by the closely attached cation.

A natural solution to alleviate the impact of a cation on such aromatic ether-based backbones is to increase the distance between the cationic functional group and the backbone (i.e., to design pendant-type APEs). As clearly indicated in Figure 5b, the degradation rate of all of the pQA-type APEs was slowed considerably. After the 30 day stability test in a 1 mol/L KOH solution at 80 °C, pQAPS, pQAPPSU, and pQAPPO all have weight losses close to 8 wt %, which is very similar to the stabilities of the pristine polymers. In other words, the pQA group has little impact on the chemical properties of the aromatic ether-based backbones, and even though the number of polar groups on the PS backbone is larger than that on the PPSU and PPO backbones, they are free from OH^- attack once the quaternary ammonia cation has been placed far enough away.

In addition to the high backbone stability, the stability of the cation in pQA-type APEs is also superior to that in the QA-type APEs. Table 1 enumerates the onset degradation temperature (T_d) of the cation group, measured by thermogravimetric analysis (TGA), showing that all pQA-type APEs have a T_d that is higher than those of the QA-type APEs. Such cation stability improvement can also be reflected in the IEC change after the aforementioned 30 day stability test. As indicated in Table 2,

Table 1. Starting Thermal Degradation Temperatures (T_d) of the Cations and Mechanical Properties for QA- and pQA-Type APEs

sample	T_d (°C)[a]	tensile strength (MPa)	elongation (%)
QAPS	168	12.99	7.23
QAPPSU	180	10.01	4.12
QAPPO	203	13.71	7.80
pQAPS	210	2.50	16.21
pQAPPSU	216	6.31	4.59
pQAPPO	214	2.83	7.32

[a] T_d was obtained from thermogravimetric analysis (TGA) for APEs with the OH^- anion.

Table 2. IEC and Ionic Conductivity (IC) of the Studied APE Membranes before and after the Stability Test in a 1 mol/L KOH Solution at 80 °C for 30 Days

	IEC (mmol/g)		IC (mS/cm, 80 °C)	
	before	after (remaining %)	before	after (remaining %)
QAPS	1.00	0.69 (69.0%)	37.5	*a*
QAPPSU	1.10	0.81 (73.6%)	40.5	*a*
QAPPO	1.35	0.96 (71.1%)	46.5	*a*
pQAPS	2.01	1.79 (89.1%)	73.7	66.4 (90.0%)
pQAPPSU	2.12	1.87 (88.2%)	83.5	74.9 (89.7%)
pQAPPO	2.23	1.90 (85.2%)	64.4	53.9 (83.7%)

[a] The ICs of QAPS, QAPPSU, and QAPPO were unmeasurable because of membrane cracking after the 30 day test.

the IEC losses of pQAPS, pQAPPSU, and pQAPPO are 10.9, 11.8, and 14.8%, respectively, which are remarkably lower than those of the QA-type APEs (31.0, 26.4, and 28.9% for QAPS, QAPPSU, and QAPPO, respectively). Because the IEC loss is small for pQAPS, pQAPPSU, and pQAPPO, it is understandable that the ionic conductivities of these pQA-type APEs drop by small degrees after the test in an 80 °C KOH solution for 30 days (Table 2). In comparison, the ionic conductivities of the QA-type APEs were no longer measurable because all of the membranes became brittle and cracked. The tensile strength of all of the pQA-type APEs is decreased to some extent (Table 1) because of phase separation in the membrane, but it is still sufficient for fuel cell applications (Figure S3 in the Supporting Information).

DOI: 10.1021/am508009z
ACS Appl. Mater. Interfaces 2015, 7, 2809−2816

CONCLUSION

After testing six APEs comprised of three types of backbones and two types of cations in a 1 mol/L KOH solution at 80 °C for 30 days, we can conclude clearly that designing pendant types of APEs is an effective approach to alleviating cation-induced degradation of aromatic ether-based backbones, such as PS, PPSU, and PPO.

Pristine PS, PPSU, and PPO are all stable in an alkaline environment. The attachment of a quaternary ammonium cation results in observed weight loss of 46, 32, and 28 wt % for QAPS, QAPPSU, and QAPPO, respectively, at the end of the 30 day test, indicating that simplifying the molecular structure of the polymer backbone barely alleviates cation-induced degradation. In contrast, moving the cation away from the backbone results in pQA-type APEs (pQAPS, pQAPPSU, and pQAPPO) that exhibit significantly improved stability with weight loss after the 30 day test of only 8 wt %, which is close to the level of the pristine polymers.

In addition to backbone stability, the pQA-type APEs also show improved cation stability and clear microphase segregation, resulting in higher ionic conductivity but lower water uptake and degrees of membrane swelling.

ASSOCIATED CONTENT

Supporting Information

A backbone degradation mechanism for QAPS, mass analysis for $[SQA^+-SQA^+Cl^-]^+$ and $[DQA^{2+}Cl^-]^+$, and the performance of H_2O_2 APEFC using a pQAPPO membrane. This material is available free of charge via the Internet at http://pubs.acs.org.

AUTHOR INFORMATION

Corresponding Authors

*E-mail: jpan@whu.edu.cn.
*E-mail: lzhuang@whu.edu.cn.

Notes

The authors declare no competing financial interest.

ACKNOWLEDGMENTS

This work was financially supported by the National Basic Research Program (2012CB215503, 2012CB932800), the National Natural Science Foundation of China (21125312, 21303124, 21303123), the Doctoral Fund of Ministry of Education of China (20110141130002), and the Fundamental Research Funds for the Central Universities (2014203020206).

REFERENCES

(1) Jacobson, M. Z.; Colella, W. G.; Golden, D. M. Cleaning the Air and Improving Health with Hydrogen Fuel-Cell Vehicles. *Science* **2005**, *308*, 1901−1905.
(2) Hickner, M. A.; Ghassemi, H.; Kim, Y. S.; Einsla, B. R.; McGrath, J. E. Alternative Polymer Systems for Proton Exchange Membranes (PEMs). *Chem. Rev.* **2004**, *104*, 4587−4612.
(3) Steele, B. C. H.; Heinzel, A. Materials for Fuel-Cell Technologies. *Nature* **2001**, *414*, 345−352.
(4) Chen, Y.; Guo, R.; Lee, C. H.; Lee, M.; McGrath, J. E. Partly Fluorinated Poly(arylene ether ketone sulfone) Hydrophilic-Hydrophobic Multiblock Copolymers for Fuel Cell Membranes. *Int. J. Hydrogen Energy* **2012**, *37*, 6132−6139.
(5) Li, G.; Pan, J.; Han, J.; Chen, C.; Lu, J.; Zhuang, L. Ultrathin Composite Membrane of Alkaline Polymer Electrolyte for Fuel Cell Applications. *J. Mater. Chem. A* **2013**, *1*, 12497−12502.
(6) Mamlouk, M.; Horsfall, J. A.; Williams, C.; Scott, K. Radiation Grafted Membranes for Superior Anion Exchange Polymer Membrane Fuel Cells Performance. *Int. J. Hydrogen Energy* **2012**, *37*, 11912−11920.
(7) Wang, X.; Li, M.; Golding, B. T.; Sadeghi, M.; Cao, Y.; Yu, E. H.; Scott, K. A Polytetrafluoroethylene-quaternary 1,4-diazabicyclo-[2.2.2]-octane Polysulfone Composite Membrane for Alkaline Anion Exchange Membrane Fuel Cells. *Int. J. Hydrogen Energy* **2011**, *36*, 10022−10026.
(8) Yamada, K.; Yasuda, K.; Fujiwara, N.; Siroma, Z.; Tanaka, H.; Miyazaki, Y.; Kobayashi, T. Potential Application of Anion-Exchange Membrane for Hydrazine Fuel Cell Electrolyte. *Electrochem. Commun.* **2003**, *5*, 892−896.
(9) Shin, D. W.; Kang, N. R.; Lee, K. H.; Cho, D. H.; Kim, J. H.; Lee, W. H.; Lee, Y. M. Proton Conducting, Composite Sulfonated Polymer Membrane for Medium Temperature and Low Relative Humidity Fuel Cells. *J. Power Sources* **2014**, *262*, 162−168.
(10) Pan, J.; Lu, S.; Li, Y.; Huang, A.; Zhuang, L.; Lu, J. High-Performance Alkaline Polymer Electrolyte for Fuel Cell Applications. *Adv. Funct. Mater.* **2010**, *20*, 312−319.
(11) Hibbs, M. R.; Hickner, M. A.; Alam, T. M.; McIntyre, S. K.; Fujimoto, C. H.; Cornelius, C. Transport Properties of Hydroxide and Proton Conducting Membranes. *Chem. Mater.* **2008**, *20*, 2566−2573.
(12) Asazawa, K.; Yamada, K.; Tanaka, H.; Oka, A.; Taniguchi, M.; Kobayashi, T. A Platinum-Free Zero-Carbon-Emission Easy Fuelling Direct Hydrazine Fuel Cell for Vehicles. *Angew. Chem., Int. Ed.* **2007**, *46*, 8024−8027.
(13) Varcoe, J. R.; Slade, R. C. T. Prospects for Alkaline Anion-Exchange Membranes in Low Temperature Fuel Cells. *Fuel Cells (Weinheim, Ger.)* **2005**, *5*, 187−200.
(14) Lu, S.; Pan, J.; Huang, A.; Zhuang, L.; Lu, J. Alkaline Polymer Electrolyte Fuel Cells Completely Free From Noble Metal Catalysts. *Proc. Natl. Acad. Sci. U.S.A.* **2008**, *105*, 20611−20614.
(15) Gu, S.; Sheng, W.; Cai, R.; Alia, S. M.; Song, S.; Jensen, K. O.; Yan, Y. An Efficient Ag−Ionomer Interface for Hydroxide Exchange Membrane Fuel Cells. *Chem. Commun. (Cambridge, U.K.)* **2013**, *49*, 131−133.
(16) Varcoe, J. R.; Slade, R. C. T.; Wrightand, G. L.; Chen, Y. Steady-State dc and Impedance Investigations of H_2/O_2 Alkaline Membrane Fuel Cells with Commercial Pt/C, Ag/C, and Au/C Cathodes. *J. Phys. Chem. B* **2006**, *110*, 21041−21049.
(17) Park, J. S.; Park, S. H.; Yim, S. D.; Yoon, Y. G.; Lee, W. Y.; Kim, C. S. Performance of Solid Alkaline Fuel Cells Employing Anion-Exchange Membranes. *J. Power Sources* **2008**, *178*, 620−626.
(18) Poynton, S. D.; Kizewski, J. P.; Slade, R. C. T.; Varcoe, J. R. Novel Electrolyte Membranes and Non-Pt Catalysts for Low Temperature Fuel Cells. *Solid State Ionics* **2010**, *181*, 219−222.
(19) Pan, J.; Li, Y.; Han, J.; Li, G.; Tan, L.; Chen, C.; Lu, J.; Zhuang, L. A Strategy for Disentangling the Conductivity−Stability Dilemma in Alkaline Polymer Electrolytes. *Energy Environ. Sci.* **2013**, *6*, 2912−2915.
(20) Matsumoto, K.; Fujigaya, T.; Yanagi, H.; Nakashima, N. Very High Performance Alkali Anion-Exchange Membrane Fuel Cells. *Adv. Funct. Mater.* **2011**, *21*, 1089−1094.
(21) John, J.; Hugar, K. M.; Meléndez, J. R.; Kostalik, H. A., IV; Rus, E. D.; Wang, H.; Coates, G. W.; Abrunã, H. D. An Electrochemical Quartz Crystal Microbalance Study of a Prospective Alkaline Anion Exchange Membrane Material for Fuel Cells: Anion Exchange Dynamics and Membrane Swelling. *J. Am. Chem. Soc.* **2014**, *136*, 5309−5322.
(22) Poynton, S. D.; Slade, R. C. T.; Omasta, T. J.; Mustain, W. E.; Escudero-Cid, R.; Ocón, P.; Varcoe, J. R. Preparation of Radiation-Grafted Powders for Use as Anion Exchange Ionomers in Alkaline Polymer Electrolyte Fuel Cells. *J. Mater. Chem. A* **2014**, *2*, 5124−5130.
(23) Li, N.; Leng, Y.; Hickner, M. A.; Wang, C. Y. Highly Stable, Anion Conductive, Comb-Shaped Copolymers for Alkaline Fuel Cells. *J. Am. Chem. Soc.* **2013**, *135*, 10124−10133.
(24) Clark, T. J.; Robertson, N. J.; Kostalik, H. A., IV; Lobkovsky, E. B.; Mutolo, P. F.; Abrunã, H. D.; Coates, G. W. A Ring-Opening

DOI: 10.1021/am508009z
ACS Appl. Mater. Interfaces 2015, 7, 2809−2816

Metathesis Polymerization Route to Alkaline Anion Exchange Membranes: Development of Hydroxide-Conducting Thin Films from an Ammonium-Functionalized Monomer. *J. Am. Chem. Soc.* **2009**, *131*, 12888−12889.
(25) Gu, S.; Cai, R.; Luo, T.; Chen, Z.; Sun, M.; Liu, Y.; He, G.; Yan, Y. A Soluble and Highly Conductive Ionomer for High-Performance Hydroxide Exchange Membrane Fuel Cells. *Angew. Chem., Int. Ed.* **2009**, *48*, 6499−6502.
(26) Varcoe, J. R.; Slade, R. C. T.; Yee, E. L. H. An Alkaline Polymer Electrochemical Interface: A Breakthrough in Application of Alkaline Anion-Exchange Membranes in Fuel Cells. *Chem. Commun. (Cambridge, U.K.)* **2006**, 1428−1429.
(27) Han, J.; Peng, H.; Pan, J.; Wei, L.; Li, G.; Chen, C.; Xiao, L.; Lu, J.; Zhuang, L. Highly Stable Alkaline Polymer Electrolyte Based on a Poly(ether ether ketone) Backbone. *ACS Appl. Mater. Interfaces* **2013**, *5*, 13405−13411.
(28) Pan, J.; Chen, C.; Li, Y.; Wang, L.; Tan, L.; Li, G.; Tang, X.; Xiao, L.; Lu, J.; Zhuang, L. Constructing Ionic Highway in Alkaline Polymer Electrolytes. *Energy Environ. Sci.* **2014**, *7*, 354−360.
(29) Wang, L.; Hickner, M. A. Low-Temperature Crosslinking of Anion Exchange Membrane. *Polym. Chem.* **2014**, *5*, 2928−2935.
(30) Li, N.; Wang, L.; Hickner, M. Cross-Linked Comb-Shaped Anion Exchange Membranes with High Base Stability. *Chem. Commun. (Cambridge, U.K.)* **2014**, *50*, 4092−4095.
(31) Katzfuß, A.; Poynton, S.; Varcoe, J.; Gogel, V.; Storr, U.; Kerres, J. Methylated Polybenzimidazole and Its Application as a Blend Component in Covalently Cross-Linked Anion-Exchange Membranes for DMFC. *J. Membr. Sci.* **2014**, *465*, 129−137.
(32) Robertson, N. J.; Kostalik, H. A., IV; Clark, T. J.; Mutolo, P. F.; Abrunã, H. D.; Coates, G. W. Tunable High Performance Cross-Linked Alkaline Anion Exchange Membranes for Fuel Cell Applications. *J. Am. Chem. Soc.* **2010**, *132*, 3400−3404.
(33) Lin, X.; Liu, Y.; Poynton, S. D.; Ong, A. L.; Varcoe, J. R.; Wu, L.; Li, Y.; Liang, X.; Li, Q.; Xu, T. Cross-Linked Anion Exchange Membranes for Alkaline Fuel Cells Synthesized Using a Solvent Free Strategy. *J. Power Sources* **2013**, *233*, 259−268.
(34) Merle, G.; Wessling, M.; Nijmeijer, K. Anion Exchange Membranes for Alkaline Fuel Cells: A Review. *J. Membr. Sci.* **2011**, *377*, 1−35.
(35) Pan, J.; Li, Y.; Zhuang, L.; Lu, J. Self-Crosslinked Alkaline Polymer Electrolyte Exceptionally Stable at 90 °C. *Chem. Commun. (Cambridge, U.K.)* **2010**, *46*, 8597−8599.
(36) Lin, B.; Qiu, L.; Lu, J.; Yan, F. Cross-Linked Alkaline Ionic Liquid-Based Polymer Electrolytes for Alkaline Fuel Cell Applications. *Chem. Mater.* **2010**, *22*, 6718−6725.
(37) Deavin, O. I.; Murphy, S.; Ong, A. L.; Poynton, S. D.; Zeng, R.; Herman, H.; Varcoe, J. R. Anion-Exchange Membranes for Alkaline Polymer Electrolyte Fuel Cells: Comparison of Pendent Benzyltrimethylammonium- and Benzylmethylimidazolium-head-groups. *Energy Environ. Sci.* **2012**, *5*, 8584−8597.
(38) Thomas, O. D.; Soo, K. J. W. Y.; Peckham, T. J.; Kulkarni, M. P.; Holdcroft, S. A Stable Hydroxide-Conducting Polymer. *J. Am. Chem. Soc.* **2012**, *134*, 10753−10756.
(39) Zha, Y.; Miller, M. L. D.; Johnson, Z. D.; Hickner, M. A.; Tew, G. N. Metal-Cation-Based Anion Exchange Membranes. *J. Am. Chem. Soc.* **2012**, *134*, 4493−4496.
(40) Arges, C. G.; Parrondo, J.; Johnson, G.; Nadhan, A.; Ramani, V. Assessing the Influence of Different Cation Chemistries on Ionic Conductivity and Alkaline Stability of Anion Exchange Membranes. *J. Mater. Chem.* **2012**, *22*, 3733−3744.
(41) Chen, D.; Hickner, M. A. Degradation of Imidazolium- and Quaternary Ammonium-Functionalized Poly(fluorenyl ether ketone sulfone) Anion Exchange Membranes. *ACS Appl. Mater. Interfaces* **2012**, *4*, 5775−5781.
(42) Lin, X.; Wu, L.; Liu, Y.; Ong, A. L.; Poynton, S. D.; Varcoe, J. R.; Xu, T. Alkali Resistant and Conductive Guanidinium-Based Anion-Exchange Membranes for Alkaline Polymer Electrolyte Fuel Cells. *J. Power Sources* **2012**, *217*, 373−380.
(43) Arges, C. G.; Ramani, V. Two-Dimensional NMR Spectroscopy Reveals Cation-Triggered Backbone Degradation in Polysulfone-Based Anion Exchange Membranes. *Proc. Natl. Acad. Sci. U.S.A.* **2013**, *110*, 2490−2495.
(44) Fujimoto, C.; Kim, D. S.; Hibbs, M.; Wrobleski, D.; Kim, Y. S. Backbone Stability of Quaternized Polyaromatics for Alkaline Membrane Fuel Cells. *J. Membr. Sci.* **2012**, *423−424*, 438−449.

DOI: 10.1021/am508009z
ACS Appl. Mater. Interfaces 2015, 7, 2809−2816